объединенный
институт
ядерных
исследований
дубна

E1-82-510

PERIPHERAL AND CENTRAL NUCLEUS-NUCLEUS COLLISIONS AT 4.2 GeV/c PER NUCLEON

Alma-Ata—Baku—Belgrade—Bucharest—Dubna—
Kishinev—Moscow—Prague—Samarkand—Sofia—
Tashkent—Tbilisi—Ulan-Bator—Varna—Warsaw—
Yerevan Collaboration

Submitted to the XXI International Conference
on High Energy Physics (Paris, 1982)
and to the International Conference
on Nucleus-Nucleus Collisions (East Lansing,
1982); to the Zeitschrift für Physik

1982

N.Akhababian, Ts.Baatar, A.M.Baldin, J.Bartke, J.Bogdanowicz, A.P.Cheplakov, A.P.Gasparian, V.G.Grishin, I.A.Ivanovskaya, T.Kanarek, E.N.Kladnitskaya, E.Kondor, D.K.Kopylova, M.Kowalski, R.A.Kvatadze, V.B.Lyubimov, V.F.Nikitina, M.I.Soloviev, V.D.Toneev
Joint Institute for Nuclear Research, Dubna, USSR

I.Ya.Chasnikov, M.I.Izbasarov, A.Kh.Vinitsky
Institute of High Energy Physics, Kazakh Academy of Sciences, Alma-Ata, USSR

O.B.Abdinov, H.N.Agakishiev, R.R.Mekhdiev, M.K.Suleimanov
Institute of Physics, Azerbaijan Academy of Sciences, Baku, USSR

S.Backović, V.Damianović, S.Drndarević, D.Krmpotić, D.Kpić, L.Simić
Institute of Physics, Belgrade, Yugoslavia

E.Balea, O.Balea, V.Boldea, S.Hakman, T.Ponta
Central Institute of Physics, Bucharest, Romania

K.K.Gudima, Yu.P.Keloglu
Kishinev State University, Kishinev, USSR

A.I.Anoshin, I.N.Erofeeva, L.A.Didenko, S.I.Lyutov, N.N.Melnikova, V.S.Murzin, V.M.Popova, L.I.Sarycheva, L.M.Shcheglova, L.N.Smirnova, A.N.Solomin, G.P.Toneeva
Scientific Research Institute for Nuclear Physics, Moscow State University, Moscow, USSR

Z.Korbel, Z.Trka, Ya.Trkova
Charles University, Prague, Czechoslovakia

F.A.Ismatova, M.M.Muminov, I.Suvonov
Samarkand State University, Samarkand, USSR

N.Angelov, L.D.Grekova, P.Kerachev, H.Semerdzhiev, P.P.Temnikov
Institute for Nuclear Research and Nuclear Energy, Sofia, Bulgaria

S.A.Azimov, S.O.Edgorov, Sh.V.Inogamov, A.A.Yuldashev, B.S.Yuldashev
Physical and Technical Institute of the Uzbek Academy of Sciences, Tashkent, USSR

N.S.Amaglobeli, N.S.Grigalashvili, M.A.Dasaeva, Z.V.Metreveli, Yu.V.Tevzadze, M.V.Topuridze
Tbilisi State University, Tbilisi, USSR

D.Tuvdendorzh, G.Sharkhu
Institute of Physics and Technics of the Mongolian Academy of Sciences, Ulan-Bator, Mongolia

D.Armutlijsky, N.Kochnev, S.Prokopieva
Higher Machino-Electrotechnical Institute, Varna, Bulgaria

H.Białkowska
Institute of Experimental Physics, Warsaw University, Warsaw, Poland

S.G.Arakelian, G.R.Gulkanian, Z.A.Kirakosian, S.A.Korchagin, I.M.Ravinovich, V.A.Vartanian
Yerevan Physical Institute, Yerevan, USSR

1. INTRODUCTION

Nuclear physics has gained quite new possibilities for experimental studies since high energy nuclear beams have been obtained[1]. On the one hand, this is due to experimental technique advantages. In a peripheral collision of the beam nucleus with the target a number of relativistic fragments arises, having almost the same direction and velocity as the projectile. This gives us a good experimental possibility of measuring lifetimes of excited projectile fragments and their interaction cross sections, to study properties of short-lived isotopes and hyperfragments, to obtain, in fact, unique beams, etc. One can thus study various interesting processes sweeped in space and Lorentz time-dilated.

A first part of this paper deals with a measurement of interaction cross sections of multicharged carbon beam fragments. Such experiments are of considerable interest now as they provide an opportunity to observe excited fragments with abnormally large cross section and lifetimes below 10^{-10} sec.

On the other hand, nucleus-nucleus collisions at small impact parameters allow essentially multinucleon interactions to be actualized, when a considerable number of particle emission sources are created within the inner volume of a nucleus. It is also very important to study the dependence of multiple production process on the number of nucleons involved in the interaction. At small momentum transfers, comparable with Fermi motion, nucleus is well described as an assembly of nucleons. But at transfers greater than about 1 GeV/c such a notion contradicts the data. Quark degrees of freedom begin to play an important role. Previous theoretical[2] and experimental[3] studies have shown that in hadron-nucleus interactions particles are produced far beyond the kinematic limit for hadron-nucleon collisions (cumulative effect). Characteristics of such processes are scale-invariant and are determined by local properties of hadronic matter. The shapes of secondary particle spectra become universal, independent neither of the atomic weight of the target nucleus nor of the type of incomning or secondary particles. For soft processes, which dominate the inelastic cross section, the A-dependence of the secondary particle yield is determined by transverse sizes of the colliding objects and could be parametrized as A^{α}, where $\alpha<1$. In the case of violent collisions an enhanced or anomalous A-dependence is observed, where α tends

to values close to unity, thus reflecting a local character of the interaction.

The main aim of this experiment is to search for quark degree of freedom in nucleus-nucleus collisions at high energies. In this paper we present data on central collisions of carbon nuclei and multinucleon collisions of protons, deuterons, helium and carbon nuclei with tantalum at 4.2 GeV/c nucleon.

It is worth mentioning that to study such a complex multiple production process as nucleus-nucleus interaction, it is very advantageous to use bubble-chamber facilities, enabling us to obtain quite a detailed picture of interaction. As it will be shown below, not only soft processes but also hard processes wit a momentum transfer of >1 GeV/c can be studied by means of bubble-chamber technique.

Some experimental results obtained recently by the 2 m JINR propane bubble-chamber collaboration are presented in this paper. The chamber with an internal tantalum target was exposed to protons at (2÷10) GeV/c, deuterons, helium and carbon at (2÷5) HeV/c nucleon. Our experimental data on interaction cross sections for inelastic nuclear collisions [4-6], on charged secondary multiplicities [5-12], on cumulative π^- production [13-15], on particle emission region dimensions [5,16], on correlated emission of π^--meson systems [15,17], and also preliminary results on anomalous cross sections [18] of carbon projectile multicharged fragments have been published elsewhere.

2. ANOMALOUS CROSS SECTIONS

In recent experiments [19-21] enhanced cross sections for interactions of projectile nuclear fragments (with $Z \geq 3$) with emulsion nuclei have been observed. Oxygen, argon and iron nuclear beams with a kinetic energy of ~ 2 GeV per nucleon were used in [19,20] while in [21] emulsion stacks were exposed in cosmic rays. It was observed that within the range of a few centimeters from the origin of the fragments their interaction cross section are appreciably higher than those which can be evaluated from the available experimental data on the cross sections for interactions of accelerated nuclei, having charges $2 \leq Z \leq 26$, with emulsion. The authors of ref. [22] conclude that the effect vanishes at a primary energy of $T_0 \sim 1$ GeV/nucleon. However, in a cosmic ray experiment [23] no evidence of the effect was found. Research in this direction started in the 50-ies [24], but up till now the situation is ambiguous. All the experiments were performed using emulsion technique.

We studied [18] this phenomenon using films taken from the 2 m propane bubble chamber exposed to a beam of carbon nuclei at 4.2 GeV/c per nucleon. Interaction cross sections for the carbon

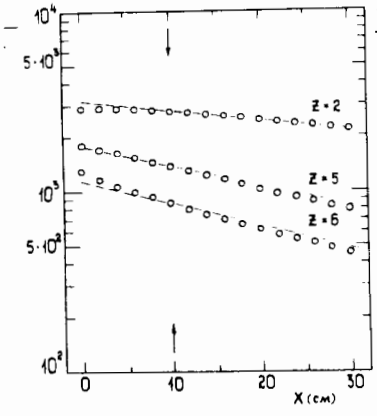

Fig. 1. Dependence of the number of noninteracting carbon projectile fragments on the distance X from the primary vertex.

projectile fragments with $Z \geq 2$ were measured within different ranges from the points of their origin. For the fragments with $Z=6$ an appreciable increase of the cross section was observed within a range of 7 cm from the origin. But for the fragments with $Z=2$ the cross section was observed to decrease. An analysis of the experimental data shows that there are certain experimental complications due to the overlapping of tracks and stars produced by different fragments coming out of the same primary interaction.

In this paper we present data on interactions of the fragments with charges $Z=5,6$. A fragment charge was determined by δ-electron density and by evaluation of the total charge of the stripping-like particles emitted from the primary star and from all relevant secondary ones [18,25]. Positively charged particles with momenta $P_+ \geq 3$ GeV/c emitted at angles $\theta \leq 4°$ with respect to the beam direction were taken as stripped ones. Figure 1 shows the dependence of the number of fragments, which have escaped interaction, on the distance X away from the primary vertex, i.e., the rate of attenuation of the beam as a function of the thickness of the target. A similar dependence for doubly charged fragments is taken from a previous paper [18] based on four times smaller statistics. The arrows indicate a boundary ($X = 10$ cm) below which the scanning and fragment identification are not reliable.

The experimental points to the right from the boundary $X = 10$ cm are consistent with a single exponential. The dashed lines correspond to an expected rate of attenuation of the beam for the fragments, which was evaluated from the experimental cross sections for interactions of primary protons, deuterons, helium and carbon nuclei in propane [14]. The curves are normalized to the observed number of fragments at the distance $X=10$ cm. For fragments with $Z=6$ the slope of the dashed line corresponds to the experimental value of the cross section for a beam carbon nucleus interaction with propane, i.e., it shows the upper limit of the slope for nonexcited fragments with $Z=6$. The lines for $Z=2$ and $Z=5$ fragments include small corrections to the experimental values of cross sections for beam helium and carbon nuclei interactions with propane.

From data in Fig.1 it follows that the values of the interaction cross sections of carbon fragments with $Z=5,6$ are ~10% greater than expected. This fact is presumably indicative of a contribution of excited fragments with a lifetime of $\tau \geq 10^{-10}$ sec the size of which becomes greater than that of the fragments in the ground state. It is worthwhile to note here that targets with smaller atomic weights are more expedient for the detection of deviations (if any) of interaction cross sections from those expected for the ground state fragments. It is known that inelastic cross sections for two nuclei depend mainly on the sum of their geometric dimensions. From this point of view emulsion nuclei are too large as compared to propane (C_3H_8) to observe small changes in fragment dimensions.

3. $^{12}C+^{12}C$ CENTRAL COLLISIONS

For central multinucleon CC collisions the following selection criteria were chosen: a) there are no carbon projectile spectator fragments with charge $Z \geq 2$; b) the number of singly charged stripped projectile fragments $n_s \leq 2$; c) the total charge of secondary particles $Q > 7$.

From 12 000 carbon-propane interactions, scanned according to the above selection criteria, 876 events were selected. According to experimental estimates, the average number of interacting nucleons in these events is 15 with a standard deviation of $\sigma \sim 3$. The selected multinucleon CC collisions are approximately symmetric. To extract protons and heavier baryons from all positive particles, we used the following procedure. In the range of positive particle momenta $P_+ \leq 500$ MeV/c protons were well distinguished from π^+ mesons by ionization density. For positive particles with $P_+ > 500$ MeV/c weights depending on momentum and angle were introduced. These weights were calculated to take into account the π^+ meson contribution estimated from the π^- meson one.

According to the multinucleon CC interaction selection criteria, only singly charged spectator fragments may be present in the projectile fragmentation region. In the target fragmentation region the energy of the spectator fragments like d, t or He is not high enough to produce a detectable track with $\ell \gtrsim 3$ mm in propane. Protons were detected starting from a momentum of $P_p \geq 150$ MeV/c.

It should also be noted that we have observed about 70 positive particles with momenta of $P_+ \geq 1$ GeV/c and a mean emission angle of $\langle\theta\rangle \simeq 35°$, which had ionization losses considerably higher than those for protons with $P_+ \geq 1$ GeV/c. Such particles were considered as deuterons, tritons and helium nuclei without separation. The fraction of spectator deuterons and tritons

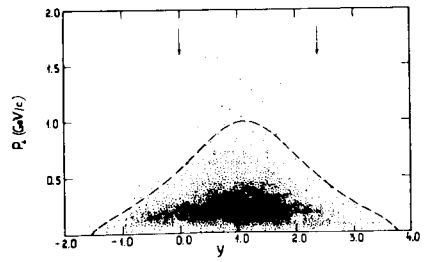

Fig.2. Plot of transverse momentum vs rapidity for π^- mesons produced in central C+C interactions. The dashed line denotes the NN kinematic limit.

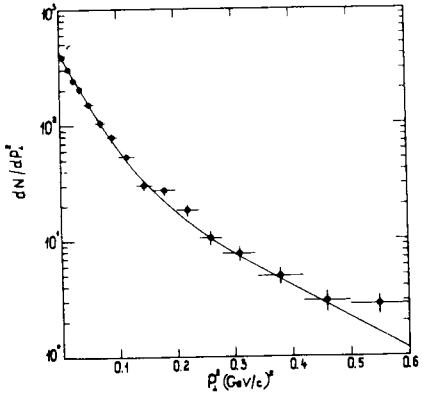

Fig.3. Transverse momentum squared distribution for π^- mesons in central C+C collisions.

from the incoming carbon nuclei and of heavy particles identified by ionization turned out to be ~5% of all charged baryons.

Shown in Fig.2 are π^+ mesons plotted in the plane of transverse momentum ($P_\perp$) and rapidity ($y = 0,5 \ln[(E+P_\parallel)/(E-P_\parallel)]$). The kinematic limit for NN collisions at 4.2 GeV/c is shown as a dashed line. Rapidities of the projectile and target are shown with arrows. A densely populated area is seen in the region near the c.m.s. rapidity $y = 1.1$ for NN collisions and at small transverse momenta. In the target rapidity region a certain loss of π^- mesons (~2% according to our estimates) is seen. Outside the kinematic boundary π^- mesons are observed predominantly in the central rapidity region. The points are distributed slightly asymmetrically due to the selection criteria for CC central multinucleon collisions. According to these criteria, we select events where, on average, a larger number of nucleons interact from the projectile nucleus than from the target.

The transverse momentum squared distribution of π^--mesons is presented in Fig.3. The horizontal bars indicate the $P_\perp^2$ experimental resolution. The experimental points were fitted by a sum of two exponentials

$$dN/dP_\perp^2 = Ae^{-aP_\perp^2} + Be^{-bP_\perp^2}. \qquad (1)$$

The result of the approximation is shown as a solid line. The slopes found are: $a = (23.1 \pm 1.8)$ $(GeV/c)^{-2}$, $b = (6.2 \pm 0.9)$ $(GeV/c)^2$, while $\chi^2/N.D.F. = 1.18$. The slope parameters for CC collisions on-

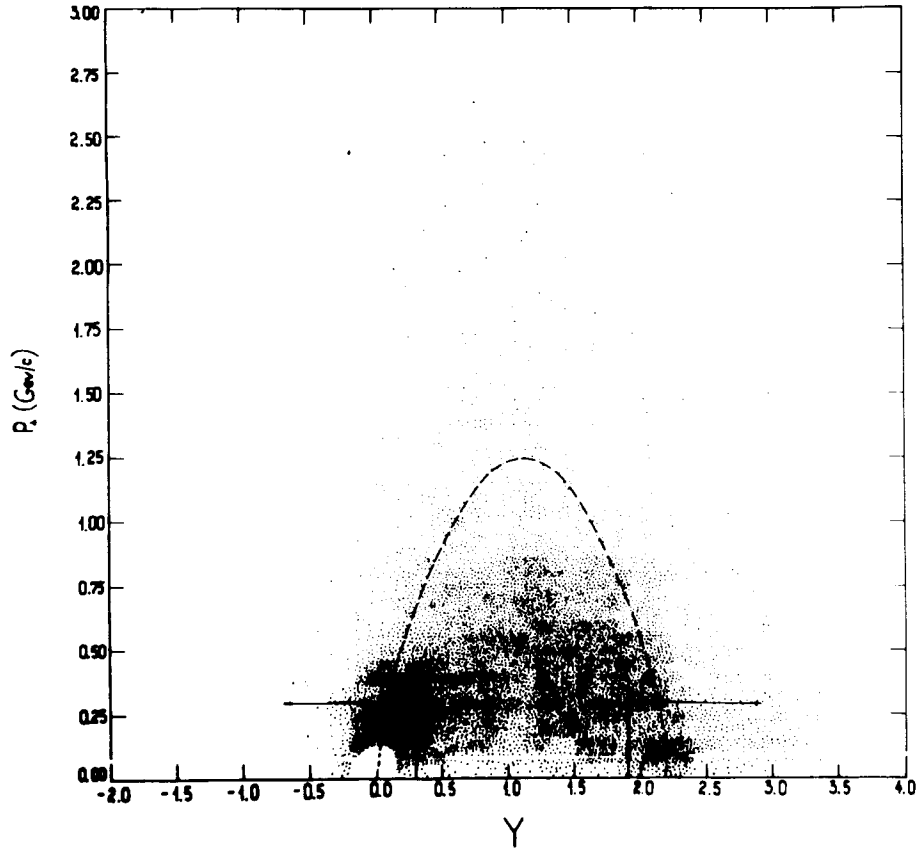

Fig.4. Plot of transverse momentum vs rapidity for protons produced in central C+C interactions. The dashed line corresponds to the NN kinematic limit.

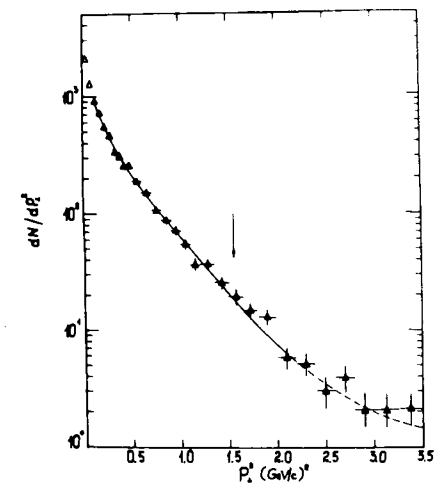

Fig.5. Transverse momentum squared distribution of protons in central C+C collisions. The arrow points to the NN kinematic limit.

ly slightly differ from those for NN collisions[26] at similar beam momentum. But the relative contribution of the second exponential is higher: 33% as compared to 23% in NN interactions.

A similar two-dimensional plot for protons is presented in Fig.4. All charged baryons were considered as protons. The kinematic limit for NN collisions is shown as a dashed line. The solid lines with arrows denote approximately the expected regions for spectator fragments of projectile and target. An apparent systematic loss of protons with $P_p \lesssim 150$ MeV/c, which have a range of less than 3 mm in propane, is seen in the target rapidity region. A concentration of experimental points corresponding to the spectator protons from carbon target is also seen. In the projectile fragmentation region the increase of point density is insignificant due to the inefficiency of the selection criteria for multinucleon CC collisions. The values of the total momenta of spectator deuterons and tritons are essentially higher than those of stripping protons. Thus the values of their rapidities calculated with proton mass are considerably greater than that of the projectile nucleus rapidity. However it is seen that even outside the projectile and target fragmentation regions the plot is to some extent asymmetric. This is again due to the selection criteria as explained for π^- mesons in Fig.2.

An interesting aspect is that quite a number of protons fall outside the NN kinematically allowed region.

The $P_\perp^2$ distribution for all protons is shown in Fig.5. At small transverse momenta of $P_\perp^2 < 0.1$ $(GeV/c)^2$, where systematic losses and the inefficiency of CC multinucleon event selection are essential, the experimental points are shown as open triangles. The horizontal error bars indicate the $P_\perp^2$ experimental resolution. The arrow points to the kinematic limit for NN interactions. The experimental data were parametrized as

$$dN/P_\perp^2 = Ae^{-aP_\perp^2} + Be^{-bP_\perp^2} + Ce^{-cP_\perp^2}. \qquad (2)$$

The slope parameters were found to be:

$$a = (8.7 \pm 1.3)\ (GeV/c)^{-2}\ ,\quad b = (2.4 \pm 0.2)\ (GeV/c)^{-2}\ ,$$
$$c = (0.2 \pm 0.8)\ (GeV/c)^{-2}. \qquad (3)$$

The result of the fit is shown as a solid line (χ^2/N.D.F.=0.81). In the high $P_\perp^2$ region the result of the approximation is shown as a dashed line reflecting an uncertainty of the third slope parameter.

Figure 5 illustrates well the main processes of proton emission. The maximum slope (open triangles) corresponds to fragmentation processes with some contamination of peripheral NN colli-

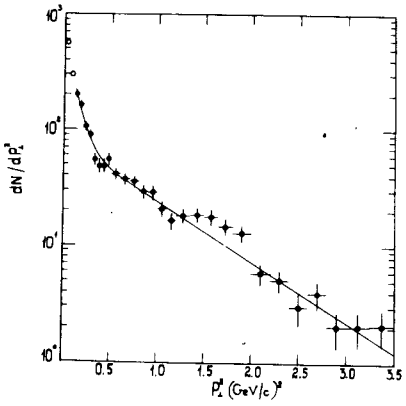

Fig.6. Transverse momentum squared distribution of those protons in central C+C collisions which fall outside the NN kinematically allowed region in the $(y, P_\perp)$ plot.

sions. The value of the second slope ~9 $(GeV/c)^{-2}$ indicates a considerable contribution of NN elastic scattering. The third slope can be treated as a manifestation of NN inelastic collisions. The decrease of the slope at $P_\perp^2$ greater than the NN kinematic limit is still to be explained.

Figure 6 presents the $P_\perp^2$ distribution for protons falling outside the NN kinematic limit in Fig.4 (dashed line). The open circles correspond to the region where the nucleus fragmentation processes are essential. The experimental distribution was approximated by a sum of two exponentials of Eq.(1). The result of this approximation is shown as a solid line (χ^2/N.D.F.=1.07). The following slope parameter values were found

$$a=(11.8\pm2)\ (GeV/c)^{-2}\ ,\quad b=(1.2\pm0.1)\ (GeV/c)^{-2}. \qquad (4)$$

As is seen from Fig.6, there is a distinct break in the slope of the distribution near $P_\perp^2 \sim 0.5\ (GeV/c)^2$. Another structure is possibly seen in the vicinity of $P_\perp^2 \sim 1\ (GeV/c)^2$.

Attention is also called to a small value of the second exponential slope ~ 1 $(GeV/c)^{-2}$. Such a value of the slope parameter corresponds to proton production processes in hard collisions at small distances.

It is interesting to study collective characteristics of secondary particles in multinucleon interactions. Different models[27-30] for nucleus-nucleus collisions predict different configuration of events in phase space which one fails to analyze in terms of single-particle inclusive distributions. For given CC central collisions the analysis of jet production of secondary particles is made by means of collective variable sphericity,

$$S=3/2\min\left(\sum_i P_{\perp i}^2 / \sum_i \vec{P}_i^{\,2}\right). \qquad (5)$$

Here $P_{\perp i}^2$ is the transverse momentum of a secondary particle relative to a certain axis, which is chosen so that the sum $\sum_i P_{\perp i}^2$ over all charged particles in an event should be minimal. This axis is a jet axis on the assumption of two-jet structure of the events. The $\vec{P}_i$ vectors are the secondary particle momenta

in the c.m.s. of the colliding carbon nuclei. This variable is calculated by diagonalization of a matrix built of the components of secondary particles momenta in the CC c.m.s. frame, which coincides with the NN c.m.s. frame. A similar analysis was done for all inelastic CC collisions extracted from experimental $C(C_3H_8)$ collisions.

While investigating the jet structure of CC interactions, multicharged fragments of the projectile nucleus as well as singly charged stripping particles were excluded. Besides, protons with a laboratory momenta of $P_p \leq 300$ MeV/c were excluded because in this region the contamination of evaporation protons from target nucleus is large. We analyzed CC interactions with a charged multiplicity of $n_{ch} \geq 4$.

The sphericity value distributions for CC interactions are shown in Fig.7. The calculation according to an intranuclear cascade model[27] taking into account the experimental restrictions is also shown here by a histogram. It is seen that the jet-like behaviour of all secondary particles in complete CC interactions agrees well with the cascade model. The mean values of sphericity in the experiment and in the model are respectively equal to $\langle S_{expt}\rangle = 0.356\pm0.009$, $\langle S_{mod}\rangle = 0.371$. Central CC collisions demonstrate higher sphericity $\langle S_{expt}\rangle = 0.477\pm0.006$ than all CC interactions, and they are not described by the intranuclear cascade model. The mean value of sphericity in the model turned out to be $\langle S_{mod}\rangle = 0.412$.

For multinucleon interactions the dimensions of secondary pion emission region were determined by the like-particle interferometry method[31]. In the case of CC central collisions the space size of π^- meson emission region appeared to be r = = (3.10±0.89) fm. It is worth to note here that interference effects are observed for particles with small four-momentum differences. At our incident energy, low energy π^- mesons are mainly produced. Therefore the size of the emission region is determined by processes with the production of just these π^- mesons. Of more interest should be a measurement of space-time characteristics of interactions where two high $P_\perp$ π^- mesons are detected.

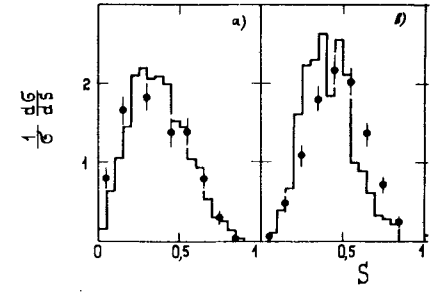

Fig.7. Sphericity distribution for C+C events. The histogram shows calculations according to the intranuclear cascade model: a) for all C+C interactions; b) for central C+C interactions.

4. INTERACTIONS WITH HEAVY NUCLEUS

A target consisting of three tantalum plates 1 mm thick was placed inside the bubble chamber. Experimental details were published elsewhere[13,32-34]. The data sample consists of 769 pTa, 1331 dTa, 780 HeTa and 1176 CTa inelastic interactions. It is possible to estimate to what extent an interaction is multinucleonic from the experimental data on the rise of secondary particle multiplicity, and of the average numbers of interacting protons depending on the atomic numbers of incoming nuclei, and from theoretical calculations[12].

For all inelastic (p,d,He,C)Ta interactions the average number of interacting nucleon pairs is approximately equal to 4,7,12 and 27, respectively. For CTa central collisions, when in the forward cone ($\theta \leq 4^\circ$) positively charged particles with momenta of $P_+ \geq 3$ GeV/c are completely absent, the average number of nucleon-nucleon interacting pairs amounts to 50. Such events consist of many charged particles, and this leads to considerable difficulties in data handling procedure. Therefore measurements were performed for all particles in an event except positively charged baryons with momenta of $P_+ \leq 700$ MeV/c.

Figure 8 presents the two-dimensional π^- distribution of transverse momentum versus rapidity for CTa interactions. The kinematic limit for NN collisions at 4.2 GeV/c is shown as a dashed line. In the target rapidity region a loss of π^- mesons (according to our estimate ~5%) is seen. A considerable asymmetry in the point distribution is connected with the fact that a larger number of nucleons interact on behalf of tantalum nucleus than from carbon nucleus. Quite a number of π^- mesons fall outside the NN kinematic boundary.

The differential cross sections of π^- mesons produced in (circles) and in dTa (triangles) interactions versus the transverse momentum squared are presented in Fig.9. The experimental points were approximated by a function (1). The result of the approximation is shown as solid lines, $\chi^2/\text{N.D.F.} = 0.96$ (CTa) and $\chi^2/\text{N.D.F.} = 0.87$ (dTa). The slope parameters of the exponentials were found to be equal to: $a = (45.4 \pm 2.8)$ $(\text{GeV/c})^{-2}$, $b = (8.3 \pm 0.4)$ $(\text{GeV/c})^{-2}$ for CTa and $a = (43.8 \pm 4.4)$ $(\text{GeV/c})^{-2}$, $b = (7.8 \pm 0.8)$ $(\text{GeV/c})^{-2}$ for dTa interactions. The relative contributions of the second exponential are 47% for CTa and 41% for dTa interactions. As is seen, the values of the slope parameters of the second exponentials in NN, dTa, CTa and CC central interactions turned out to be similar. A large difference in the values of the slope parameters of the first exponentials seems to be connected with the contribution of π^- mesons produced in the interactions of secondary nucleons in tantalum.

The invariant π^- meson spectra were analyzed also in terms of A and $P_\perp$. It is known[3,35-37] that the ratio of π^- meson

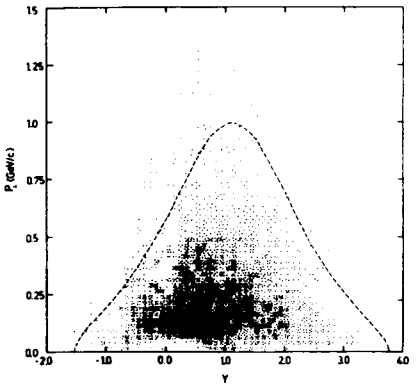

Fig.8. Plot of transverse momentum vs rapidity for π^- mesons produced in C+Ta interactions. The dashed line represents the NN kinematic limit.

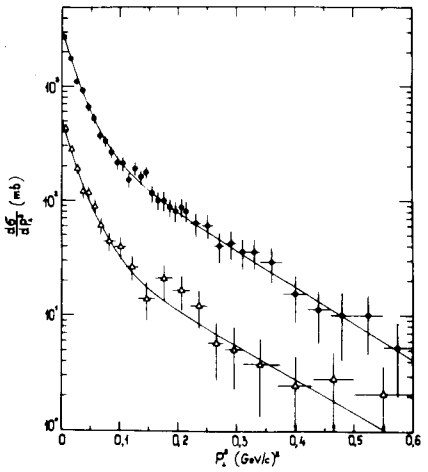

Fig.9. π^- meson yields vs transverse momentum squared in C+Ta (circles) and in d+Ta (triangles) interactions.

structure functions in pA and pp interactions obeys the power-like A-dependence

$$R = (E d^3\sigma/d^3p)_{pA} / (E d^3\sigma/d^3p)_{pp} = A^{\alpha(p_\perp)}, \qquad (6)$$

where $\alpha(p_\perp)$ is a universal rising function of transverse momentum independent of atomic number A, and at high $p_\perp$ its values become equal to 1.1÷1.3. Search and investigation of such anomalous A-dependences are of great importance for testing and development of present-day quark models[38,39].

To study the A-dependence of π^- meson structure functions in our experiment, it is natural to suggest that parametrization (6) may be generalized directly for nucleus-nucleus interactions

$$R_{A_1B_1/A_2B_2} = (E d^3\sigma/d^3p)_{A_1B_1} / (E d^3\sigma/d^3p)_{A_2B_2} = (A_1B_1/A_2B_2)^{\alpha(p_\perp)}, \qquad (7)$$

where A_1, A_2 and B_1, B_2 are atomic numbers of projectile and target nuclei, respectively. In our case the ratios of π^- meson structure functions over $p_\perp$ in (d,He,C)Ta interactions to the corresponding distributions in pTa interactions were studied. We investigated also analogous ratios with the dTa data in the dominator. Let us denote the ratios with pTa data in the

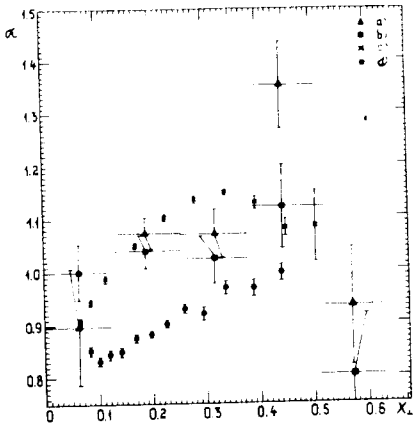

Fig.10. Dependence $a(x_\perp)$ for π^- structure function ratios: a) for $R_{A/p}$ values; b) for $R_{A/d}$ values; c) $a(x_\perp)$ in pA interactions at 400 GeV/c; d) $a(x_\perp)$ in pA interactions at 70 GeV/c.

Fig.11. Plot of transverse momentum vs rapidity for positive particles with momenta of $P_+ \geq 700$ MeV/c in C+Ta interactions. The dashed line corresponds to the NN kinematic limit.

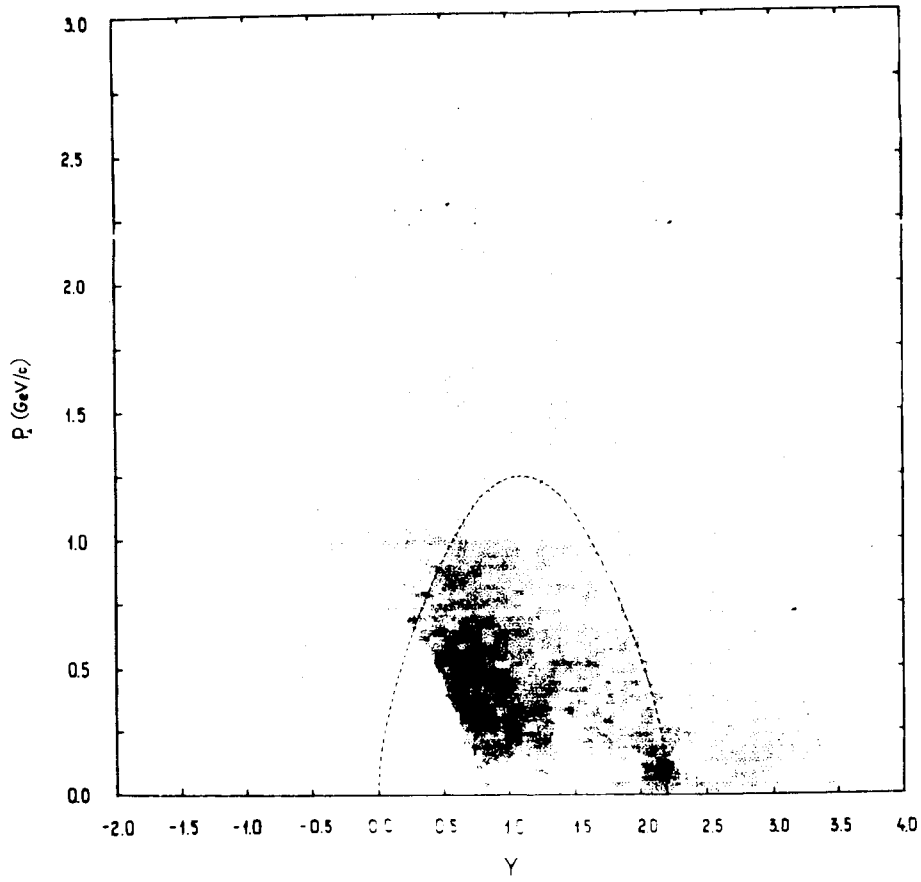

dominator as $R_{A/p}$, and those with dTa data as $R_{A/d}$. Experimental ratios $R_{A/p}$ (and $R_{A/d}$) were jointly fitted for different intervals of transverse momentum.

Figure 10 presents the obtained $a(x_\perp)$ dependences for the ratios of the π^- structure functions $R_{A/p}$ and $R_{A/d}$, where $x_\perp = 2P_\perp/\sqrt{s}$. Similar dependences, obtained in pA-collisions at 400 GeV/c [37] and 70 GeV/c [40], are also shown. It is seen that due to low statistics the errors of the values of parameter a are large. In the interval $0.2 \lesssim x \lesssim 0.5$ the values of parameter $a \gtrsim 1$. This result should be considered as an indication of an anomalous A-dependence of π^- meson yield in nucleus-nucleus interactions at relatively small transverse momenta $0.2 \lesssim P_\perp \lesssim 1$ GeV/c and at not high momentum per beam nucleon.

In Fig.11 is presented a plot of $P_\perp$ versus the rapidity of positive particles with momenta of $P_+ \geq 700$ MeV/c for CTa interactions. Multicharged stripping fragments of incoming carbon nucleus are not included in this plot. The π^+ meson contamination estimated from π^- mesons amounts to 8% of all the particles in the plot. Among positive particles with $P_+ \geq 700$ MeV/c about 4% of particles with $P_+ \geq 1$ GeV/c were found having higher ionization density, which were considered as d, t, He nuclei. While calculating rapidity, all particles were classified as protons. The absence of particles with $P_+ < 700$ MeV/c is distinctly seen in Fig.11 in the tantalum nucleus fragmentation region. The dashed line corresponds to the NN kinematic limit. It is seen that a considerable part of protons falls outside the kinematic limit.

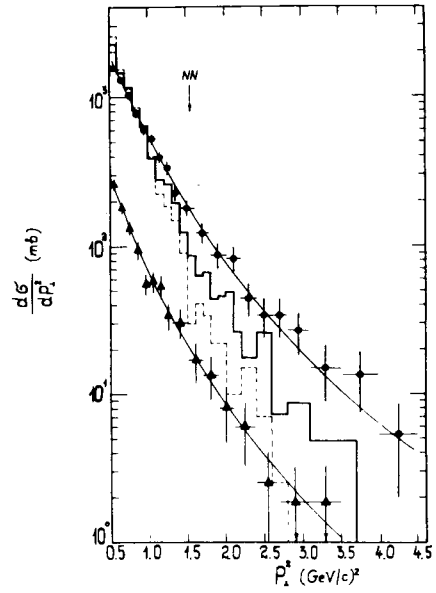

In Fig.12 are presented differential cross sections of protons produced in CTa (circles) and in dTa (triangles) interactions versus the transverse momentum squared for $P_\perp^2 \geq 0.5$ (GeV/c)^2. The π^+ meson contamination amounted to 4%. The transverse momentum squared for spectator fragments of

Fig.12. Proton yields vs transverse momentum squared for $P_\perp^2 \geq 0.5$ (GeV/c)^2. The arrow points to the NN kinematic limit. The histograms represent two versions of the intranuclear cascade model calculations for C+Ta interactions.

carbon nucleus did not exceed 0.5 $(GeV/c)^2$. Therefore if in a first approximation we neglect the yield of composite particles, then hadrons with high transverse momenta can be considered as protons. In Fig.12 the kinematic limit for NN collisions is shown with an arrow. Experimental points for (d,He,C)Ta interactions were approximated by the function (1). For pTa collisions the experimental points were approximated by a single exponential due to low statistics. The slope parameters of the exponentials for all exposures are presented in the Table.

Table

Exponential slope parameters obtained by fitting the P^2 distributions of protons in (p,d,He,C)+Ta interactions

Fitted parameters A_P	p	d	He	C
a	3.19±0.62	3.29±0.39	3.21±0.35	2.62±0.33
b	-	0.56±0.54	0.44±0.35	0.99±0.54
χ^2/N.D.F.	0.31	0.82	1.16	1.05

Figure 12 shows two versions of calculations according to the Dubna cascade model DCM[21] for CTa interactions in the form of histograms. The theoretical calculations are normalized to the experimental proton yields with $P_\perp^2 \geq 0.5$ $(GeV/c)^2$. In the first version of the model (dashed line) the secondary protons did not interact in the final state. In the second version (solid line) any two or more nucleons in an event with momenta, which differ by a value less than parameter P_0, were considered as composite particles (d,t,He). The P_0 parameter, the radius of momentum sphere for sticking together, was estimated from the secondary particle spectra in Ne+U collisions[41] at energies of 0.4÷2.1 GeV per projectile nucleon and was taken equal to 90 MeV/c. Such an approach is similar to introducing final state interactions in the coalescence model[42].

In order to reproduce the experimental conditions, all composite particles, obtained in the second version of calculations, were considered as protons. It is seen that with the final state interactions not taken into account the model does not describe the data in the region of high momentum transfers. With the coalescence introduced, the description improves, but there are still essential deviations from the experiment.

Rapidity distributions of protons with high transverse momenta for dTa and CTa interactions are presented in Fig.13 along

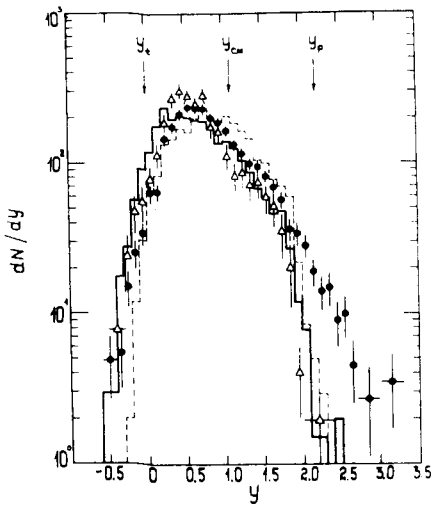

Fig.13. Rapidity distributions of protons with $P_\perp^2 \geq 0.5$ (GeV/c) for d+Ta(triangles) and for C+Ta (circles) interactions. The histograms show two versions of the intranuclear cascade model calculations.

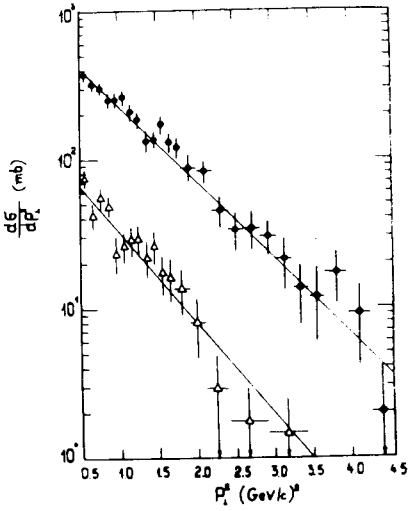

Fig.14. Proton yields vs transverse momentum squared for those protons which are located outside the NN kinematically allowed region in the $(y,P_\perp)$ plot for d+Ta (triangles) and for C+Ta(circles) interactions.

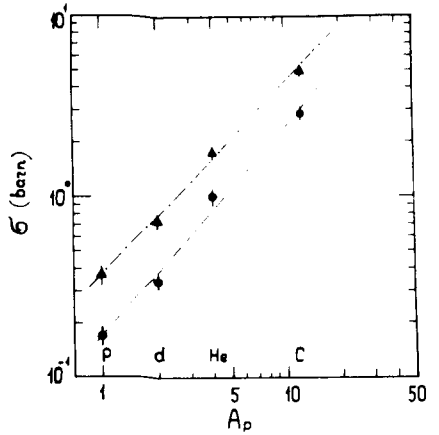

Fig.15. A-dependence of the proton yields on transverse momentum squared in the intervals $(0.5 \leq P_\perp^2 < 1.0)$ $(GeV/c)^2$ - triangles, and $P_\perp^2 \geq 1$ $(GeV/c)^2$ - circles.

with the DCM calculations. The agreement cannot be considered as satisfactory.

The $P_\perp^2$ distribution of protons falling outside the NN kinematic limit on the $(y,P_\perp)$ plot is given in Fig.14. Circles correspond to CTa interactions, while triangles represent dTa interactions. The experimental points were approximated by the function

$$d\sigma/dP_\perp^2 = Ae^{-aP_\perp^2}. \qquad (8)$$

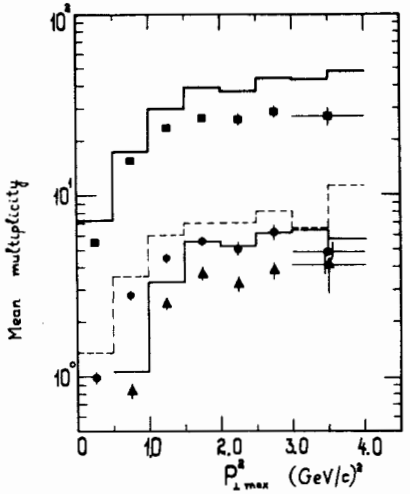

Fig.16. Average multiplicities of positive particles (squares), π^- mesons (circles) and protons with $P_\perp^2 \geq 0.5$ (GeV/c)^2 (triangles) vs maximum transverse momentum of proton in an event, $P_{\perp\,max}^2$. The lines represent the intranuclear cascade model calculations (lower line for protons, middle for pions, and upper for all positive secondaries).

The result of the approximation is shown as solid lines, χ/N.D.F. = 0.81 for dTa and χ^2/N.D.F. = 1.4 for CTa interactions. According to DCM with final state interactions, the calculations disagree with the data.

Shown in Fig.15 is the A-dependence of the proton yields in the regions of $P_\perp^2$ $(0.5 \leq P_\perp^2 < 1)$ (GeV/c)^2 (triangles) and $P_\perp^2 \geq 1$ (GeV/c)^2 (circles). The lines represent a power-like fit given by

$$\sigma = cA^\alpha \,, \qquad (9)$$

where A is the atomic weight of the projectile. For the two $P_\perp^2$ intervals $\alpha = 1.07 \pm 0.02$ and $\alpha = 1.17 \pm 0.03$, respectively. When fitting, the first point was fixed. The A-dependence becomes steeper with increasing $P_\perp^2$, and the α-values are greater than unity in both intervals.

Fig.16 shows the average multiplicities of positive particles (squares), π^- mesons (circles) and protons with $P_\perp^2 \geq 0.5$ (GeV/c)^2 (triangles) versus the maximum value of $P_\perp^2$ in the event. Predictions of DCM with proton coalescence are shown with lines. It is seen that events with high $P_\perp^2$ protons demonstrate a high charged multiplicity. Starting from the NN kinematic limit $P_\perp^2 \sim 1.5$ (GeV/c)^2, the average charged multiplicities are practically independent of $P_{\perp\,max}^2$. The cascade model qualitatively reproduces the correlation but overestimates the particle multiplicities.

For all inelastic as well as for central CTa interactions the size, r, of the π^- meson emission region was measured by the interferometry method. It was found that $r = (3.44 \pm 0.41)$ fm and $r = (4.11 \pm 1.07)$ fm for all inelastic CTa and for CTa central interactions, respectively. As is seen, the r value is determined within the statistical errors by the size of carbon projectile.

CONCLUSIONS

The experimental dependence is obtained of the cross sections for multicharged carbon beam fragment interactions with propane on the distance from the origin of these fragments. It follows from the data that the values of the interaction cross sections of carbon fragments with $Z = 5,6$ in propane at a distance of $X \gtrsim 10$ cm from the vertex are ~10% greater than those expected. It is probably an indication of the contribution of excited fragments with a life-time of $\tau \gtrsim 10^{-10}$ sec the size of which becomes greater than that of the ground state.

In multinucleon CC and (d,He,C)Ta collisions π^- mesons and protons are produced far outside the NN kinematic boundary. For secondary charged baryons a new exponential dependence on $P_\perp^2$ is observed with the value of slope parameter ~1 (GeV/c)$^{-2}$. In the A-dependence of proton yields with $P_\perp > 1$ GeV/c in the interactions of light nuclei with tantalum α is close or exceeds unity. The data are not described by a cascade model with final-state interactions included. Thus a considerable contribution of cumulative interactions is observed.

In the future an increase of statistics is planned. We also plan to study a deuteron contribution to the high $P_\perp$ region, correlations and further comparison of models with the data.

The authors are indebted to the technical staff for film taking and for assistance in data processing.

REFERENCES

1. Baldin A.M. et al. PTE, 1971, 3, p.29; JINR, P9-5442, Dubna, 1970.
2. Baldin A.M. JINR, P7-5808, Dubna, 1971; Brief Comm. on Phys., 1971, 1, p.35; Progress in Particle and Nuclear Physics, 1980, 4, p.95.
3. Baldin A.M. et al. JINR, P1-5819, Dubna, 1971; Proc. Rochester Meeting APS/OPF, N.Y., 1971, p.131; Stavinsky V.S. ECHAYA, 1979, 10, p.949.
4. Akhababian N. et al. JINR, 1-12114, Dubna, 1979; Gasparian A.P. et al. JINR, 1-12797, Dubna, 1979.
5. Angelov N. et al. Z.Physik C, 1980, 5, p.1.
6. Angelov N. et al. Yad.Fiz., 1981, 33, 4, p.1046.
7. Angelov N. et al. Yad.Fiz., 1978, 27, 4, p.1020.
8. Angelov N. et al. JINR, E1-11517, Dubna, 1978; Yad.Fiz., 1978, 28, 5, p.1304.

9. Angelov N. et al. Yad.Fiz., 1979, 30, 6, p.1590.
10. Baatar Ts. et al. Yad.Fiz., 1980, 32, 5, p.1372.
11. Baatar Ts. et al. JINR, P1-80-209, Dubna, 1980.
12. Gasparian A.P. et al. Yad.Fiz., 1981, 34, 5, p.1328.
13. Agakishiev H.N. et al. Yad.Fiz., 1981, 34, 6, p.1517.
14. Baatar Ts. et al. JINR, P1-81-516, Dubna, 1981.
15. Agakishiev H.N. et al. INR, 1904/VI/PH/A, Warsaw,1981.
16. Angelov N. et al. Yad.Fiz., 1980, 31, 2, p.411.
17. Akhababian N. et al. JINR, E1-81-470, Dubna, 1981.
18. Agakishiev H.N. et al. JINR, P1-81-79, Dubna, 1981.
19. Friedlander E.M. et al. Phys.Rev.Lett., 1980, 45, p.1084.
20. Jain P.L., Das G. Phys.Rev.Lett., 1982, 48, p.305.
21. Barber H.B. et al. Phys.Rev.Lett., 1982, 48, p.856.
22. Aggarwal M.M. et al. Proc. of the Fifth Heavy-Ion Conf., University of California at Berkeley, 18-22 May, 1981; Phys.Lett.B, 1982, 112, p.31.
23. Freier P.S., Waddington C.J. Astrophys.Space Sci., 1975, 38, p.419.
24. Judek B. Can.J.Phys., 1968, 46, p.343; Gleghorn T.F. et al. Can.J.Phys.Suppl., 1968, 46, p.572.
25. Gasparian A.P., Grigalashvili N.S. JINR, 1-11335, Dubna, 1979.
26. Abdivaliev A. et al. JINR, P1-81-437, Dubna, 1981.
27. Gudima K.K., Toneev V.D. JINR, P2-10431, Dubna, 1977; Yad.Fiz., 1978, 27, p.658.
28. Gugnon J. Phys.Rev., 1980, C22, p.1885.
29. Stöcker H. et al. Phys.Rev.Lett., 1980, 44, p.725.
30. Kapusta J., Strottman. Phys.Rev., 1981, C23, p.1282.
31. Kopylov G.I., Podgoretsky M.I. Yad.Fiz., 1973, 18, p.656; JETP, 1975, 69, p.414.
32. Angelov N. et al. Yad.Fiz., 1980, 32, p.1582.
33. Angelov N. et al. JINR, 1-12424, Dubna, 1979.
34. Gasparian A.P. et al. JINR, 1-80-778, Dubna, 1980.
35. Cronin J.W. et al. Phys.Rev.D., 1975, 11, p.3105.
36. Kluberg L. et al. Phys.Rev.Lett., 1977, 38, p.670.
37. Antreasyan D. et al. Phys.Rev.D, 1979, 19, p.764.
38. Zmushko V.V. Yad.Fiz., 1980, 32, p.448.
39. Treleani D., Wilk G. Nuovo Cim. A, 1980, 60, p.201.
40. Abramov V.V. et al. Yad.Fiz., 1980, 31, p.660.
41. Sandoval A. et al. Phys.Rev.C, 1980, 21, p.1321.
42. Gutbrod H.H. et al. Phys.Rev.Lett., 1976, 37, p.667; Gosset J. et al. Phys.Rev.C., 1977, 16, p.629; Lemaire H.C. Phys.Lett.B, 1979, 85, p.38.

Received by Publishing Department
on July 2 1982.

SUBJECT CATEGORIES OF THE JINR PUBLICATIONS

Index	Subject
1.	High energy experimental physics
2.	High energy theoretical physics
3.	Low energy experimental physics
4.	Low energy theoretical physics
5.	Mathematics
6.	Nuclear spectroscopy and radiochemistry
7.	Heavy ion physics
8.	Cryogenics
9.	Accelerators
10.	Automatization of data processing
11.	Computing mathematics and technique
12.	Chemistry
13.	Experimental techniques and methods
14.	Solid state physics. Liquids
15.	Experimental physics of nuclear reactions at low energies
16.	Health physics. Shieldings
17.	Theory of condenced matter
18.	Applied researches
19.	Biophysics

Ахабабян Н. и др. E1-82-510

Периферические и центральные ядро-ядерные столкновения при 4,2 ГэВ/с/нуклон

Представлен экспериментальный материал по взаимодействию релятивистских ядер p , d , ^{4}He , ^{12}C с ядрами углерода и тантала, полученный с помощью 2-метровой пропановой пузырьковой камеры с внутренней мишенью из тантала. Установлено, что сечения взаимодействия вторичных фрагментов налетающих ядер углерода с зарядом $Z = 5,6$ на 10% больше ожидаемой величины. В пятнадцатинуклонном столкновении ядер углерода и многонуклонных взаимодействиях ядер d , ^{4}He , ^{12}C с танталом наблюдается вклад коллективных взаимодействий, не сводящихся к суперпозиции NN -столкновений с учетом ферми-движения, взаимодействия в конечном состоянии, перерассеяний и т.д.

Работа выполнена в Лаборатории высоких энергий ОИЯИ.

Препринт Объединенного института ядерных исследований. Дубна 1982

Akhababian N. et al. E1-82-510

Peripheral and Central Nucleus-Nucleus Collisions at 4.2 GeV/c per Nucleon

Experimental data on interactions of relativistic p , d ,He and C nuclei with carbon and tantalum nuclei are presented. The data come from the 2 m propane bubble chamber with an internal tantalum target. It is found that interaction cross sections for carbon projectile fragments with charges $Z=5,6$ are 10% greater than expected. In central C+C collisions and in multinucleon interactions of d , He and C with tantalum a contribution is observed from cumulative interactions irreducible to the superposition of NN -collisions taking into account final state interactions, rescattering effects, etc.

The investigation has been performed at the Laboratory of High Energies, JINR.

Preprint of the Joint Institute for Nuclear Research. Dubna 1982